

# PREDICTION AND VALIDATION OF CHAOTIC BEHAVIOR IN AN ELECTROSTATICALLY ACTUATED MICROELECTROMECHANICAL OSCILLATOR

B.E. DeMartini, H.E. Butterfield, J. Moehlis, and K.L. Turner

<sup>1</sup>Department of Mechanical Engineering, University of California, Santa Barbara, United States  
(Tel : (805) 893-7849; E-mail: baredog@umail.ucsb.edu)

**Abstract:** We investigate chaotic behavior for a microelectromechanical (MEM) oscillator, which is modeled by a version of the Mathieu equation that contains both linear and nonlinear time varying stiffness coefficients. By using Melnikov's method we have developed a criterion for the existence of chaos in such oscillators, which depends solely on system parameters. Chaotic behavior was observed experimentally and numerically for a MEM oscillator developed using the criterion from our analysis.

**Keywords:** chaos, Melnikov's method, nonlinear dynamics, parametric resonators

## 1. INTRODUCTION

Many physical systems have the ability to exhibit chaotic behavior. Perhaps the most famous example is the Lorenz equations [1], which have helped to understand the dynamics of cellular convection. Recently, chaos has been reported for various nonlinear MEM oscillators [2-5]. We investigate the existence of chaos for a class of nonlinear parametrically excited MEM oscillators that has recently been studied [6,7] and proposed for applications such as mass sensing [8] and signal filtering [9].

In order for these complex nonlinear devices to be utilized in real world applications, it is important to understand the conditions (system parameters) that result in chaotic behavior. The ability to predict such behavior is not only useful for designing robust devices with predictable dynamics (i.e. for the applications listed above), but also for applications such as signal encryption [3] that exploit chaotic vibrations.

## 2. PREDICTIVE ANALYSIS

Characteristic to the class of oscillators studied herein are linear and cubic nonlinear time varying stiffness coefficients arising from the electrostatic actuation mechanism. These coefficients lead to abrupt changes in dynamic behavior (nearly instantaneous jumps from a stable quiescent state to a stable oscillator state), when the excitation frequency is near  $2\omega_0/n$  (where  $n$  is an integer greater than or equal to 1), which make them attractive for applications such as those discussed in Section 1. A MEMS that exhibits this type of

behavior, shown in Figure 1, consists of noninterdigitated combdrive actuators (AC and DC), suspending flexures (K), and a shuttle mass (M) [7-9].

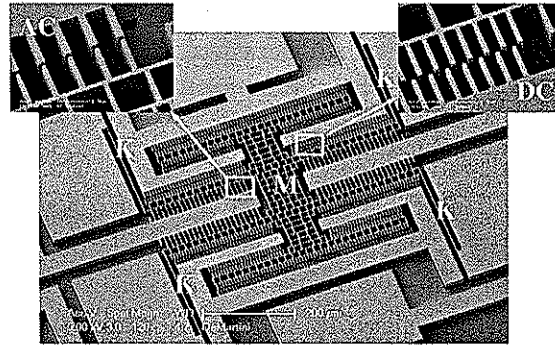


Fig.1 SEM image of the chaotic oscillator.

The two sets of noninterdigitated combdrives are used for periodic excitation (AC) and for DC tuning (DC) [9-11] and generate an electrostatic force  $F_{es}(x,t) = (r_{10}x + r_{30}x^3)V_0^2 + (r_{1A}x + r_{3A}x^3)V(t)^2$ , where  $r_{10}$  and  $r_{30}$  are electrostatic stiffness coefficients corresponding to the tuning combdrive,  $r_{1A}$  and  $r_{3A}$  are electrostatic stiffness coefficients corresponding to the excitation combdrive,  $V_0$  is the voltage amplitude applied to the DC combdrive, and  $V(t) = V_A(1 + \cos(\omega t))^{1/2}$  is the signal applied to the AC combdrive (decouples parametric and harmonic excitation [6]) with amplitude  $V_A$ . The mechanical flexures (K) generate a force,  $F_f(x) = (k_1x + k_3x^3)$ , where  $k_1$  and  $k_3$  are stiffness coefficients. Including a dissipative force due to damping in the system, the

nondimensional equation of motion is

$$z'' + \alpha z' + \beta z + \delta z^3 + \gamma(1 + \cos \Omega \tau) z + \eta(1 + \cos \Omega \tau) z^3 = 0 \quad (1)$$

where  $\omega_0 = (k_1/m)^{1/2}$ ,  $\tau = \omega_0 t$  (scaled time),  $\Omega = \omega/\omega_0$  (scaled driving frequency),  $' = d/d\tau$ ,  $z = x/x_0$  (scaled displacement, where  $x_0$  is a characteristic length),  $\alpha = c/(\omega_0 m)$  ( $c$  is the damping coefficient),  $\beta = 1 + r_{10} V_0^2/k_1$ ,  $\delta = x_0^2(k_3 + r_{30} V_0^2)/k_1$ ,  $\gamma = r_{1A} V_A^2/k_1$ ,  $\eta = x_0^2 r_{3A} V_A^2/k_1$ .

In this analysis we use an analytical technique, Melnikov's method [12], to deduce the presence of chaos in Equation (1). In order to apply Melnikov's method to this system, the parameters are rescaled. First, parameters corresponding to time dependent and velocity terms ( $\alpha, \gamma$ , and  $\eta$ ) are assumed to be small (much less than 1), which is a valid assumption for MEM oscillators. In other words, they are considered perturbations to the Hamiltonian system,  $z'' + \beta z + \delta z^3 = 0$ . Second, the other parameters ( $\beta$  and  $\delta$ ) are assumed to be order one quantities. A necessary condition for this analysis is that the unperturbed Hamiltonian system must contain a double well potential, which requires

$$\beta < 0, \quad \delta > 0. \quad (2)$$

Taking these assumptions into account, Melnikov analysis [12] was applied to determine the following criterion for the existence of chaos

$$\left| 3\alpha |\beta|^{3/2} \delta \sinh \left( \frac{\pi \Omega}{2\sqrt{|\beta|}} \right) \right| < \left| \pi \Omega^2 (6\delta\gamma + \eta(4|\beta| + \Omega^2)) \right|. \quad (3)$$

An oscillator, governed by Equation (1), whose system parameters satisfy this expression will have a chaotic invariant set, which may or may not be an attractor.

### 3. VERIFICATION OF CHAOS

Both numerical and experimental investigations that verify the above criterion for the existence of chaos are presented in this section.

Using Equations (2) and (3) as criteria for the parameters of the system, an oscillator was designed to exhibit chaotic behavior. In order to satisfy  $\beta < 0$  for a range of  $V_0$ , the tuning combdrives must be designed such that  $r_{10} < 0$ , since  $k_1$  is always positive. Since  $k_3$  is also always positive (mechanical flexures are naturally hardening),  $\delta > 0$  can be satisfied either by having

$r_{30} < 0$  or  $r_{30} > 0$ . Note, for the case where  $r_{30} > 0$ ,  $\delta > 0$  will be true for all  $V_0$ . To satisfy these conditions, fixed-fixed flexures (with relatively large  $k_3$ ) and misaligned noninterdigitated combdrives for DC tuning were chosen. See [10,11] for discussions on how alignment and geometry affect the sign of combdrive stiffness coefficients. Using aligned noninterdigitated combdrives for AC excitation ( $r_{1A} > 0$  and  $r_{3A} < 0$ ) Equation (3) is satisfied for a range of  $V_A$ ,  $V_0$ ,  $\omega$ ,  $m$ , and  $c$  ( $x_0 = 1$  used throughout analysis). Note Equation (3) can also be satisfied for a variety of AC excitation combdrive configurations, i.e. for a variety of  $r_{1A}$  and  $r_{3A}$  sign combinations.

The theoretical parameters for the chaotic oscillator, which was fabricated using standard silicon on insulator processing [13] (device shown in Figure 1), are

$$r_{10} = -4.7e-3 \text{ } [\mu\text{N}/(\text{V}^2 \mu\text{m})], \quad r_{30} = 1.8e-4 \text{ } [\mu\text{N}/(\text{V}^2 \mu\text{m}^3)], \\ r_{1A} = 1.1e-3 \text{ } [\mu\text{N}/(\text{V}^2 \mu\text{m})], \quad r_{3A} = -1.4e-4 \text{ } [\mu\text{N}/(\text{V}^2 \mu\text{m}^3)], \\ k_1 = 9.6 \text{ } [\mu\text{N}/\mu\text{m}], \quad k_3 = 7.3 \text{ } [\mu\text{N}/\mu\text{m}^3], \quad m = 1.6e-9 \text{ } [\text{kg}].$$

The electrostatic coefficients were determined using finite element software. An estimate of the quality factor was determined experimentally in a 535 mTorr vacuum environment, which is consistent throughout all experiments, to be  $Q = 1558$ . These estimated parameters were used in numerical simulations for comparison with the experimental results.

A DC voltage was applied to the tuning electrodes, with no AC excitation, and was slowly increased. When  $V_0$  was large enough, the topology of the potential energy became a double well and small fabrication induced asymmetries and noise caused device to buckle to one of the new equilibrium positions. Figure 2 shows the buckling event observed in the experiment.



Fig. 2 Microscope snapshots of a pair of combfingers ( $V_0$  shown below each image). Their relative position demonstrates the buckling event.

Notice that the onset of buckling occurs somewhere between  $V_0 = 36\text{V}$  and  $36.5\text{V}$ , which is apparent by the relative position of the combfingers.

To test the dynamics of the oscillator when a

square root cosine signal was applied to the set of AC excitation fingers, a Polytec laser vibrometer was used [11]. For this experiment a DC signal, which is above 36.5V, is applied to the tuning fingers while simultaneously applying the square root cosine signal to the other set. The parameters  $V_A$ ,  $V_0$ , and  $\omega$  were varied and the output signal from the laser vibrometer was analyzed using an oscilloscope. Above  $V_0 = 36.5V$  the qualitative behavior of the oscillator changes drastically, which was also seen in numerical simulations.

Numerous points in parameter space ( $V_A, V_0, \omega$ ) where attracting chaotic behavior exists have been found. For instance, for  $V_0 = 37.1V$ ,  $V_A = 13.8V$ , and  $\omega/2\pi = 2000Hz$ , sustainable chaos exists, which is depicted in Figure 3a. Observing the velocity signal over a long period of time, no repeated behavior was observed, and the amplitude of the signal was several orders of magnitude greater than the noise floor, suggesting that this was indeed chaotic behavior.

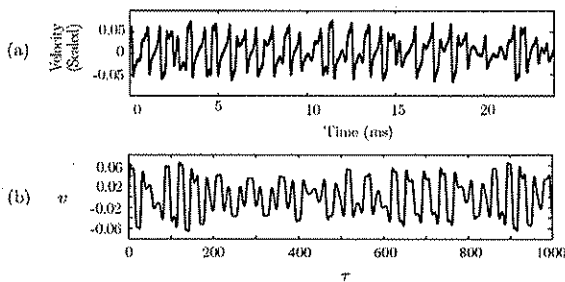


Fig. 3 Chaotic time series found (a) experimentally with  $V_A = 13.8V$ ,  $V_0 = 37.0V$ , and  $\omega/2\pi = 2000Hz$  (1 velocity (scaled) unit = 125 mm/s) and (b) numerically with  $V_A = 15.0V$ ,  $V_0 = 46.5V$ , and  $\omega/2\pi = 2010Hz$  ( $v=z'$  is nondimensional velocity where  $z=x/x_0$ ).

Using the theoretical parameters discussed above sustainable chaos was found numerically for  $V_A = 15.0V$ ,  $V_0 = 46.5V$ , and  $\omega/2\pi = 2010Hz$ , which are reasonably close to the experimental parameters. The resulting velocity time series shown in Figure 3b shows the chaotic behavior and provides further proof that the experimental result was in fact chaotic.

Analyzing the spectral content of the oscillator's time series is a good indicator of whether or not the behavior is chaotic. This was

done by taking the modulus of Fourier transform of the velocity time series obtained experimentally and numerically, for the same  $V_A, V_0$ , and  $\omega$  used in Figure 3. Figure 4 a and b show respectively the power spectra from experiment and numerical simulation.

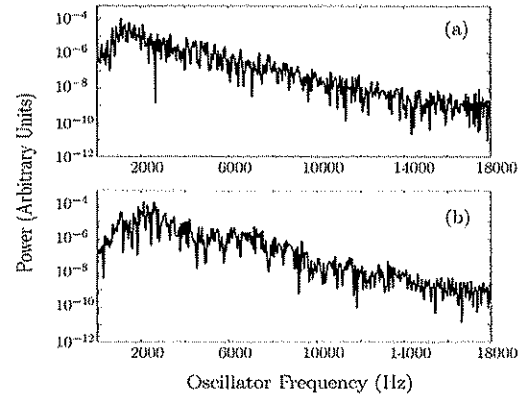


Fig. 4 Broadband power spectrum of a chaotic attractor found (a) experimentally and (b) numerically for the same parameters as Figure 3 (the velocity units prior to taking the Fourier transform are identical to Figure 3 (a) and (b)).

The broadband power spectrum seen in both panels of Figure 4 is characteristic of chaos. Also, both experimental and numerical power spectra look strikingly similar.

A boundary, in  $\omega/2\pi - V_A$  space, above which chaos is predicted to occur, has been derived from Equation (3). Figure 5 shows the boundary for two DC voltages (dashed and dotted curves).

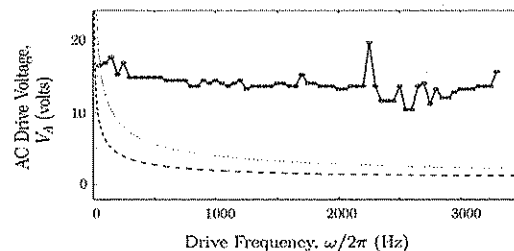


Fig. 5 Boundaries above which attracting chaos is found in experiment (solid curve  $V_0=37.0V$ ) and chaos is predicted by Equation (3) (dashed curve:  $V_0=47.0V$  and dotted curve:  $V_0=37.0V$ ).

A boundary has also been measured

experimentally by fixing  $V_0=37.0V$ , increasing  $V_A$  until attracting chaotic behavior was observed, and recording this  $V_A$  every 50 Hz. Note, only voltages below  $V_A=25.0V$  were applied to the device, since similar devices failed for voltages slightly above this value. The important result here is that the experimental boundary lies above the theoretical boundaries. It is therefore concluded that Equation (3) is a good predictive tool for chaos in this type of MEM oscillator.

### 3. CONCLUSION

Melnikov's method has been used to analytically predict the existence of chaos in a MEM oscillator, which is governed by a nonlinear version of the Mathieu equation. The criterion resulting from this analysis is an inequality that is useful for designing an oscillator's parameters so that chaos either occurs or does not occur as desired. Using this criterion, an electrostatically actuated and tuned MEM oscillator has been designed to exhibit chaotic behavior. An experiment was set up, using a laser vibrometer to track the vibration of the shuttle mass, and by tuning various system parameters ( $V_A, V_0, \omega$ ), chaos was found. Using the estimated system parameters numerical simulations for nearby  $V_A, V_0$ , and  $\omega$ , sustainable chaos was also found. In conclusion, the criterion from Melnikov's method is a valid tool for predicting the existence of chaos for the type of oscillator studied herein.

### ACKNOWLEDGEMENTS

The authors would like to thank the National Science Foundation (NSF-0428916 and NSF-0547606) for supporting this research and Steve Shaw and Jeff Rhoads for informative discussions.

### REFERENCES

- [1] E. Lorenz, "Deterministic nonperiodic flow", *J. Atm. Science*, Vol. 20, pp. 130-141, 1963.
- [2] M. Basso, L. Giarre, M. Dahleh, and I. Mezic, "Numerical analysis of complex dynamics in atomic force microscopes", *IEEE Intl. Conf. on Control. Apps.*, Trieste, Italy, 1-4 September, 1998.
- [3] Y. Wang, S. Adams, J. Thorp, N. MacDonald, P. Hartwell, and F. Bertsch, "Chaos in MEMS, parameter estimation and its potential application", *IEEE Trans. on Circ. and Syst.*, Vol. 45, No. 10, pp. 1012-1020, 1998.
- [4] S. Liu, A. Davidson, and Q. Lin, "Simulation Studies on nonlinear dynamics and chaos in a MEMS cantilever control system", *J. Micromech. and Microengr.*, Vol. 14, pp. 77-83, 2004.
- [5] A. Luo and F. Wang, "Nonlinear dynamics of a micro-electro-mechanical system with time-varying capacitors", *J. Vib. and Acoust.*, vol. 126, pp. 77-83, 2004.
- [6] K. Turner, S. Miller, P. Harwell, N. MacDonald, S. Strogatz, and S. Adams, "Five parametric resonances in a microelectromechanical system", *Nature*, Vol. 396, pp. 149-152, 1998.
- [7] J. Rhoads, S. Shaw, K. Turner, J. Moehlis, B. DeMartini, and W. Zhang, "Generalized parametric resonance in electrostatically-actuated microelectromechanical oscillators", *J. Sound and Vib.*, Vol. 296, pp. 797-829, 2006.
- [8] W. Zhang, R. Baskaran, and K. Turner, "Effect of nonlinearity on auto-parametrically amplified resonant MEMS mass sensor", *Sens. and Act. A-Phys.*, Vol. 103 No. 1-2, pp. 139-150, 2002.
- [9] J. Rhoads, S. Shaw, K. Turner, and R. Baskaran, "Tunable MEMS filters that exploit parametric resonance", *J. Vib. and Acoust.*, Vol. 127, No. 5, pp. 423-430, 2004.
- [10] S.G. Adams, F.M. Bertsch, K.A. Shaw, and N.C. MacDonald, "Independent tuning of linear and nonlinear stiffness coefficients," *J. MEMS*, Vol. 7, No. 2, pp. 172-180, 1998.
- [11] B. DeMartini, J. Rhoads, K. Turner, S. Shaw, and J. Moehlis, "Linear and nonlinear tuning of parametrically excited MEM oscillators", In Press, *J. MEMS*, 2007.
- [12] J. Guckenheimer and P. Holmes, *Nonlinear Oscillators, Dynamical Systems, and Bifurcations of Vector Fields*, Springer-Verlag, New York, 1983.
- [13] W. Zhang, W. Zhang, K. Turner, and P. Hartwell, "SCREAM'03: A single mask process for high-Q single crystal silicon MEMS," *ASME Intl. Mech. Eng. Congr. on Sens.*, Vienna, Austria, 24-27 Oct. 2004.